M. Reuber
Department of Mechanical Engineering, Carleton University, Ottawa, Ontario; currently, University of Illinois at Chicago, Chicago, Ill. 60680

A. Schultz
Department of Materials Engineering, University of Illinois at Chicago, Chicago, Ill. 60680

F. Denis
St. Paul-Ramsey Medical Center, Saint Paul, Minn. 55101

D. Spencer
Department of Orthopaedic Surgery, University of Illinois Medical Center, Chicago, Ill. 60612

Bulging of Lumbar Intervertebral Disks

Lateral, posterolateral, posterior, and end plate bulges in the intervertebral disks of 14 fresh human cadaver lumbar motion segments were measured. Loads were applied in compression of up to 800 N; and in right lateral bending, extension, flexion, and torsion of up to 12 Nm. Mean disk bulges up to 2.7 mm were found. Disk bulges differed little after fluid injection or after posterior element removal.

Introduction

Transverse bulging of the intervertebral disk and longitudinal bulging of the vertebral end plates may occur when spine motion segments are subjected to mechanical loads. Bulging may be a source of pathology. A bulging disk might put pressure on an adjacent spinal nerve root, and the strain in a bulging end plate might excite end plate pain receptors. Measurements of disk and end plate bulging are also useful for the construction and validation of finite-element models employed for disk stress analyses. Lumbar motion segment behavior is of particular interest, because the lumbar region is a common site of spine pathologies.

Lumbar disk bulging in response to compression loads has been measured by Hirsch and Nachemson [4]; Brown, Hansen and Yorra [3]; Lin, Liu and Adams [6] and Shah, Hampson, and Jayson [12]. Lumbar end plate bulging in response to compression has been measured by Rolander and Blair [10]. Disk bulging in response to bending moments has been reported by Brown, et al. [3] and in response to bending moments combined with compression, by Lin, et al.[6]. The present studies were undertaken to provide more comprehensive data about lumbar disk and end plate bulging.

Lateral, posterolateral and posterior disk bulging, and longitudinal end plate bulging in response to compression, right lateral bending, flexion, extension, and torsion loads are reported here. Measurements were made in 14 fresh human cadaver lumbar motion segments.

Material and Methods

Fourteen lumbar motion segments were obtained at autopsy from nine cadavers. Autopsies were made within 24 hr after death. Eight motion segments were from males and five from females, and one was of unknown sex. Ages ranged from 42 to 67, with a mean of 57 yr. Five segments were from the L1-2, three from the L2-3, five from the L3-4, and one from the L4-5 level. Disk transverse cross-sectional areas ranged from 14 to 24 cm^2. Specimens were prepared and tested at room temperature and 100 percent relative humidity, and stored at $-20°C$. Neither cause-of-death records nor specimens roentgenographs indicated any grounds on which to suspect that specimen mechanical behaviors might be abnormal.

Specimens were mounted in a testing machine with their midtransverse plane horizontal. Epoxy embedment and mechanical clamping were used to secure the upper and lower vertebrae into the test fixtures. The lower fixture was secured to the base of the testing machine, while the upper fixture was free to move without constraint (Fig. 1).

Two vertical flexible cables attached to the upper fixture were used to apply compression loads. Two other cables attached to the upper fixture were used to apply pure moments in flexion, extension, lateral bending, or torsion, depending on cabling and test-fixture configurations. The compression loads were applied using pneumatic cylinders and sensed by load cells; the moments were applied using dead weights of known magnitudes.

The motion of the superior vertebra relative to the inferior was sensed by six machinists' dial gages. Intradiskal pressure was measured using the pressure-sensitive needle described by Nachemson and Elfstrom [8]. Transverse displacements of the intervertebral disk periphery were measured at five sites; two lateral, two posterolateral, and one posterior. The disk displacement transducers each consisted of a small diameter brass rod attached to the tip of a thin strain-gaged cantilever flexure. The free end of the rod rested on the disk surface; and

Contributed by the Bioengineering Division for publication in the JOURNAL OF BIOMECHANICAL ENGINEERING. Manuscript received by the Bioengineering Division, January 5, 1981, revised manuscript received February 23, 1982.

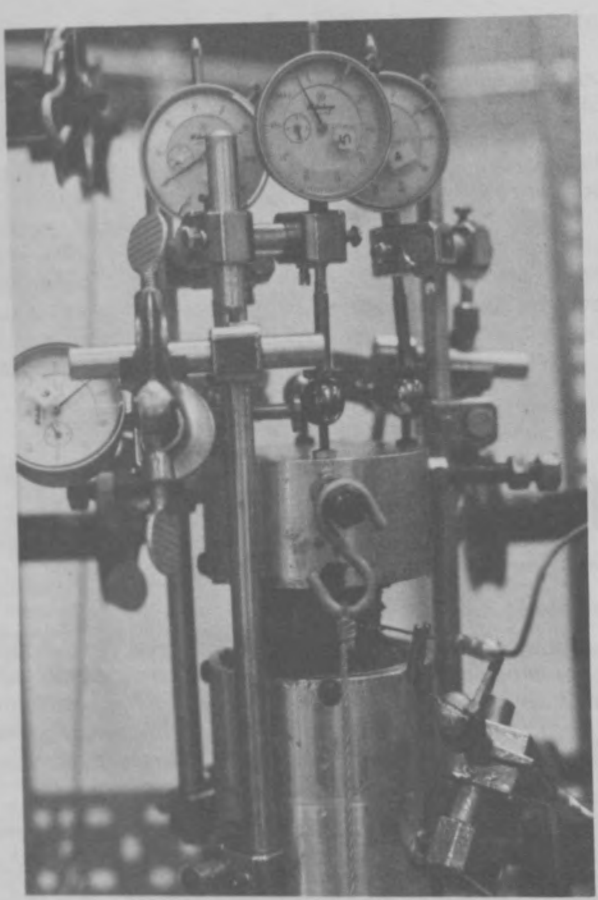

Fig. 1 Testing apparatus detail. The motion segment can be seen between the upper and lower cylindrical fixtures. The dial gage followers rest on the metal balls attached to the top of the superior fixture, and the loading arms protrude from this fixture. Loading cables are guided by the various pulleys, depending on what type of load is to be applied. The large cylinder is the inferior fixture. Clamps allow this to rotate so that different modes of loading can be applied. The bulge measuring transducers are not shown, but all bulge transducers and dial gage mounts are secured to and rotate with the inferior fixture.

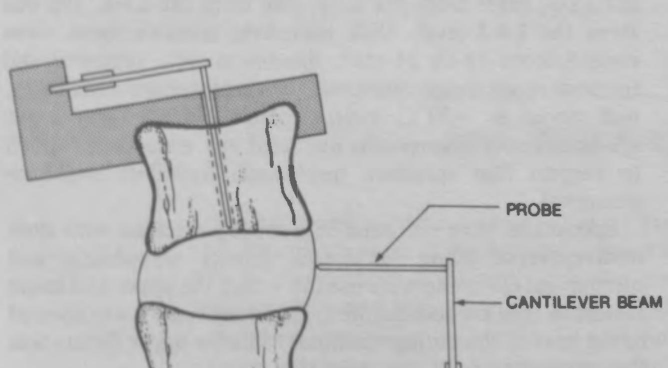

Fig. 2 Schematic diagram of the transducers used to measure transverse and end plate bulges

the flexure was oriented so that it sensed transverse displacement of that surface (Fig. 2). The posterolateral measurements sites were immediately lateral of the posterior element complex. To measure posterior disk displacement, a small diameter hole was drilled through the spinous process of the lower vertebra, allowing the sensing rod to pass through to the disk surface. Longitudinal displacement of the superior end plate was measured with a sixth displacement transducer. A small diameter hole was drilled through the center of the upper test fixture and through the center of the upper vertebral body, stopping just above the bony end plate. The sensing rod passed through this hole, to rest on the top of the upper end plate center (Fig. 2). This transducer was anchored to the superior test fixture, and so sensed superior end plate motion relative to this fixture.

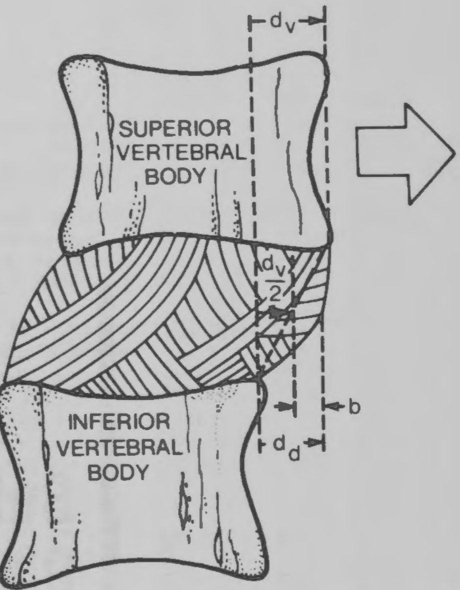

Fig. 3 Definition of disk transverse bulge when transverse relative displacements of vertebrae occur. For clarity, no vertebral tilt is shown in this schematic diagram, although it always occurred. Moreover, the diagram shows an initial bulge of zero, while the actual calculation computes the change in bulge from the initial, nonzero value.

The loading sequence began with an 800 N compression load applied in 200 N increments. The compression was then reduced to 400 N and maintained while a right-lateral bending moment of 9.8Nm was applied in four increments. These loads were removed and the loading cable configuration changed. A 400 N compression load was reapplied in a single increment and maintained while a 9.8 Nm extension moment was applied in four increments. In a similar manner, a 7.9 Nm flexion moment and then an 11.9 Nm torsional moment were applied, completing the loading sequence. The compressive preload of 400 N approximated the weight of the body segments above L3 in an average-sized adult.

Segments were next injected with isotonic saline solution to raise their no-load intradiskal pressures to three-to-six times their noninjected values. Four specimens would not retain saline. The behavior of ten saline-retaining specimens under no load was observed for 5 min, then the entire loading sequence was repeated for these ten specimens. Before application of each different mode of loading, the specimens were reinjected with saline. The facet joints and all soft-tissue connections between the posterior elements of the two vertebrae were then cut away in all 14 specimens, and the loading sequence repeated once again.

Instrument read-out began 15 s after the application of each increment of load. Significant creep seldom took place after 15 s. Data were gathered from the six dial gages sensing vertebral body motion, the six transducers sensing disk and end plate displacements, and the pressure-measuring needle. This took approximately 30 s.

After testing, all motion segments were sectioned through their midtransverse plane and graded for visual signs of degeneration according to the descriptions of Nachemson [7]. Grade 1 disks showed no signs of degeneration, while Grade 4 disks showed marked degeneration in both nucleus and annulus.

The measurements were processed by a computer program supplied with segment geometry and dial gage location data.

Table 1 Disk bulge in fluid-retaining segments before fluid injection

	Lateral bulge, mm		Posterolateral bulge, mm		Posterior bulge, mm
	Left	Right	Left	Right	
Bulge due to compression					
Compression 400 N	0.42(0.45)	0.39(0.36)	0.25(0.37)	0.13(0.47)	−0.09(0.39)
Compression 800 N	0.55(0.56)	0.55(0.28)	0.39(0.55)	0.28(0.54)	0.00(0.63)
Additional bulge due to moments					
Rt. lat. bending 3.9 Nm	−0.42(0.23)	0.39(0.17)	−0.37(0.26)	0.16(0.46)	−0.22(0.57)
Extension 3.9 Nm	−0.11(0.24)	0.12(0.22)	0.09(0.45)	0.20(0.24)	0.14(0.19)
Flexion 3.9 Nm	0.06(0.15)	−0.02(0.23)	−0.06(0.24)	−0.08(0.35)	−0.05(0.20)
Ccw. torsion 3.9 Nm	−0.07(0.14)	0.02(0.11)	−0.04(0.19)	−0.05(0.08)	−0.05(0.21)
Rt. lat bending 9.8 Nm	−0.97(0.57)	0.97(0.37)	−0.79(0.53)	0.52(0.44)	−0.35(0.61)
Extension 9.8 Nm	−0.31(0.49)	0.30(0.45)	−0.10(0.68)	0.32(0.31)	0.04(0.61)
Flexion 7.9 Nm	0.19(0.26)	−0.08(0.43)	−0.01(0.40)	−0.14(0.44)	−0.11(0.38)
Ccw. torsion 11.9 Nm	−0.23(0.38)	0.00(0.19)	−0.05(0.29)	−0.11(0.24)	−0.07(0.53)

Standard deviations are given in parentheses. 10 Nm corresponds to approximately 5 deg of tilt for all modes of tilting. In torsion 10 Nm corresponds to approximately 2 deg of twist.

Table 2 Disk bulge in nonfluid-retaining segments

	Lateral bulge, mm		Posterolateral bulge, mm		Posterior bulge, mm
	Left	Right	Left	Right	
Bulge due to compression					
Compression 400 N	0.66(0.43)	0.57(0.50)	0.61(0.60)	0.62(0.37)	−0.24(0.32)
Compression 800 N	0.80(0.30)	0.80(0.59)	0.76(0.61)	0.80(0.42)	0.34(0.26)
Additional bulge due to moments					
Rt. lat. bending 3.9 Nm	−0.79(0.67)	0.83(0.65)	−0.92(0.83)	0.30(0.26)	−0.49(0.62)
Extension 3.9 Nm	−0.03(0.46)	−0.10(0.59)	0.21(0.59)	0.14(0.16)	0.24(0.41)
Flexion 3.9 Nm	−0.07(0.74)	0.05(0.85)	−0.48(1.94)	−0.47(0.92)	−0.73(2.49)
Ccw. torsion 3.9 Nm	−0.05(0.26)	−0.04(0.17)	−0.09(0.14)	−0.27(0.43)	−0.04(0.65)
Rt. lat bending 9.8 Nm	−2.11(2.41)	−2.11(2.41)	−2.15(2.29)	0.72(1.22)	−1.13(1.38)
Extension 9.8 Nm	−0.13(0.84)	−0.14(1.13)	0.07(1.13)	0.11(0.26)	0.21(0.78)
Flexion 7.9 Nm	−0.21(1.21)	0.16(1.48)	−0.82(1.95)	−0.63(0.41)	−1.11(1.73)
Ccw. torsion 11.9 Nm	0.21(1.19)	−0.58(0.89)	−0.29(0.19)	−1.01(2.07)	−0.67(2.30)

Standard deviations are given in parentheses. 10 Nm corresponds to approximately 5 deg of tilt for all modes of tilting. In torsion 10 Nm corresponds to approximately 2 deg of twist.

The three translations of the approximate center of the superior vertebral body and the three rotations of the superior vertebra in response to each increment of load were calculated from the dial gage readings[1]. End plate bulge was measured directly by its transducer, but disk bulge also had to be calculated.

Disk bulge was defined as the transverse displacement of the disk surface minus one-half the transverse displacement of the superior vertebral body edge relative to the inferior in that same direction (Fig. 3). If the upper vertebra moves purely longitudinally, the disk bulge is equal to the disk surface transverse displacement. If the upper vertebra translates horizontally, disk bulge can be positive, zero, or negative, depending on the relationship between disk and vertebral body transverse motions. The disk bulge reported here in all bending and torsion modes is in addition to the bulge due to a 400 N compression preload. Moreover, only changes in bulge from the unloaded state are reported.

Means and standard deviations over the 14 specimens of all responses were computed. These numbers were also computed for the groups of saline-retaining and nonretaining specimens, and for the visual degeneration-graded groups with grades 1, 2 and 3 and 4.

Additional details concerning the specific materials and methods used here, the testing techniques in general, and the saline injection procedures may be found in the reports of Reuber [9]; Schultz, et al. [11]; and Andersson and Schultz [1], respectively.

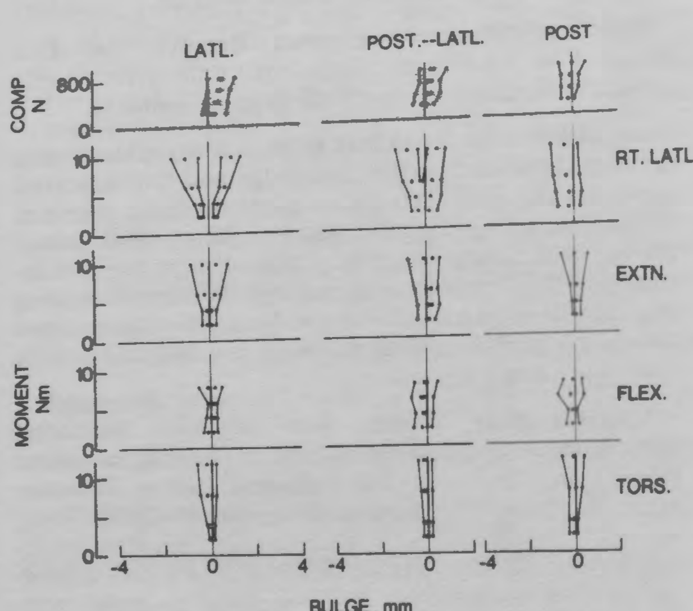

Fig. 4 Disk bulge in fluid-retaining segments before fluid injection. Mean compressive motion at 800 N was 1 mm, mean vertebral tilt values were approximately 5 deg for a 10 Nm moment in flexion, extension, or lateral bending, and mean twist was approximately 2 deg for a 10-Nm torsional moment.

[1] Geometry data measured in the unloaded segment were always used in this calculation, because under the largest loads applied, vertebral body deformations were estimated to be less than 0.05 mm. See results section for a description of this estimation procedure. The precise location of the superior vertebral body center is otherwise immaterial to the results; the dial gage readings are used to determine the movements of this point under the applied loads rather than its absolute locations.

Results

Disk Bulge in Fluid-Retaining Segments Before Fluid Injection. Only the changes in disk bulge under load are reported; unloaded-state bulges were not taken into consideration. In response to the application of a compressive preload, the mean lateral disk bulge was 0.4 mm for a 400-N load and 0.6 mm for an 800-N load (Table 1, Fig. 4).

In response to the application of bending and torsional moments, bulge in addition to that resulting from the 400 N compressive loading occurred. The largest additional bulge occurred in right lateral bending. In the mean, a 1-mm additional bulge on the right side and a − 1-mm additional bulge on the left side resulted from the application of a 9.8 Nm right lateral bending moment. Application of extension, flexion, and torsional moments up to 12 Nm produced less than ±0.5 mm of additional lateral bulge.

Posterolateral additional bulges had nearly the same magnitudes as the lateral additional bulges in all modes of applied loadings. Posterior additional bulge was less than ±0.5 mm in all modes of applied loading.

Disk Bulge in Nonfluid-Retaining Segments. Nonfluid-retaining disks showed marked increases in bulge magnitudes and in data variability compared to those for the fluid-retaining disks (Table 2, Fig. 5). The additional bulge in nonretaining disks was about twice as much as in the fluid-retaining disks in response to right lateral bending moments, for example. Nonfluid-retaining segments also exhibited larger translations and rotations than those exhibited by the fluid-retaining segments under the same loads.

Effects of Fluid Injection on Disk Bulge. Fluid-retaining specimens, upon saline injection, bulged laterally an average of 0.2 mm under a 400-N compressive preload. This was approximately half the mean bulge for 400 N before fluid injection. Posterolateral bulges showed a similar trend. Bulges in response to all other modes of applied loading were similar to those measured prior to fluid injection.

Effect of Posterior Element Removal on Disk Bulge. Posterior element removal had little effect on disk bulge in fluid-retaining or nonfluid-retaining segments.

Intradiskal Pressure and Disk Bulge. Although increasing the load increased both the disk bulge and the intradiskal pressure in any given segment, no clear relationship appeared between intradiscal pressure and disk bulge. Both lateral bending and flexion moments produced large pressure increases in fluid-retaining segments, but only lateral bending produced large bulges, for example. Fluid-retaining segments sustained higher intradiskal pressures, but bulged less than nonfluid-retaining segments.

Verterbal Body Motion. Vertebral body horizontal translations were sometimes as large as, and on occasions larger than, the largest disk transverse bulges. This was especially evident in nonfluid-retaining segments (Table 3).

End Plate Bulge. The longitudinal bulge of the bony end plate was usually much smaller than the transverse bulge of the disk (Table 4). In fact, the small apparent end plate bulges that were sensed by the transducer could have been due entirely to vertebral body compression. For the mean specimen cross-sectional area of 17 cm^2, a compressive load of 800 N corresponds to a compressive stress of approximately 50 N/cm^2. Stress-strain relations for lumbar vertebral body compression (Sonada [13]) show a compressive strain of 0.004 at this stress level. For a typical vertebral body height of 20 mm this corresponds to a height reduction of approximately 0.1 mm. This vertebral body height reduction is nearly the same as the mean value obtained for apparent end plate bulge in response to 800 N compression, so that actual end plate bulge may have been negligible.

Criteria for Degeneration. When the segment responses were grouped according to visual degeneration grades rather than fluid-retention ability, the same trends for disk bulge were found. The group of grade 1 and 2 segments behaved in nearly the same way as the group of fluid-retaining segments, and the group of grade 3 and 4 segments behaved in nearly the same way as the group of nonfluid-retaining segments. In other words, the findings regarding bulge behavior versus degeneration do not depend on which of the two criteria is used to evaluate degeneration.

More comprehensive data from the present experiments on disk and end-plate bulges, intradiskal pressures, and vertebral body motions are reported by Reuber [9].

Discussion

The chief findings of this study are: Under compressive loads up to 800 N and moments up to 11.8 Nm, mean disk

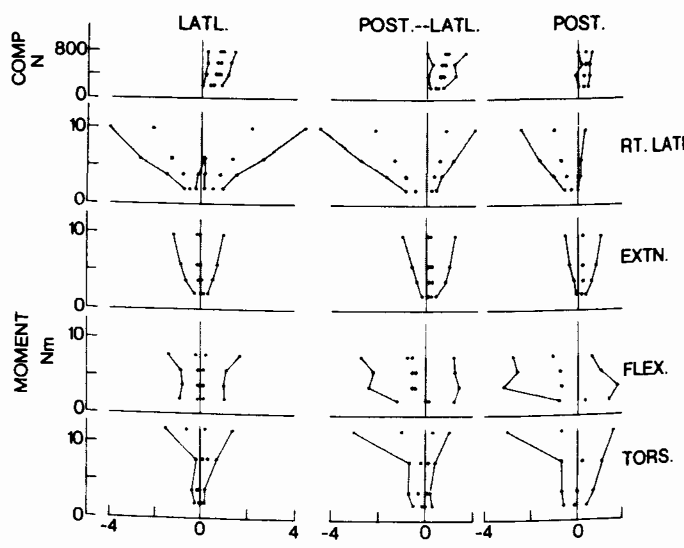

Fig. 5 Disk bulge is nonfluid-retaining sements before fluid injection. Mean compressive motion at 800 N was 1 mm, mean vertebral tilt values were approximately 5 deg for a 10-Nm moment in flexion, extension, or lateral bending, and mean twist was approximately 2 deg for a 10-Nm torsional moment.

Table 3 Vertebral body translations, mm

Translations due to compression	Fluid-retaining segments before fluid injection		Nonfluid-retaining segments	
	Left	Posterior	Left	Posterior
Compression 400 N	−0.25(0.68)	0.26(0.86)	−0.36(0.89)	−0.05(0.66)
Additional translations due to moments				
Rt. lat. bending 9.8 Nm	−0.18(0.45)	0.52(1.26)	1.07(3.88)	1.95(2.23)
Extension 9.8 Nm	0.61(0.90)	0.78(1.09)	0.28(1.43)	0.56(1.27)
Flexion 7.9 Nm	−0.20(0.54)	−0.71(1.13)	0.06(2.39)	0.50(2.67)
Ccw. torsion 11.8 Nm	0.63(0.73)	0.13(1.02)	0.21(2.28)	0.35(3.24)

Table 4 End plate bulge

		Fluid retaining segments before fluid injection, mm	Nonfluid retaining segments, mm
Bulge due to compression			
Compression 400 N		0.07(0.09)	0.07(0.08)
Compression 800 N		0.11(0.17)	0.08(0.04)
Additional bulge due to moments			
Rt. lat. bending	9.8 Nm	−0.02(0.03)	−0.03(0.01)
Extension		−0.01(0.04)	−0.11(0.21)
Flexion	7.9 Nm	0.02(0.09)	0.02(0.03)
Ccw. torsion	11.8 Nm	0.00(0.03)	−0.01(0.02)

The extension moments applied were 9.8 Nm for tests with the posterior elements intact and 7.9 Nm for tests with the posterior elements removed.

bulges of up to 2.7 mm beyond the unloaded-state bulges occur; the largest bulges are produced in right lateral bending; degenerated disks bulge more than nondegenerated disks under the same load; fluid injection and posterior element removal do not affect bulge appreciably; and end plate bulge is small compared to disk bulge. We assume that these results reflect mechanical behavior in vivo. We did not measure bulge in response to direct shear loadings.

Most of the segments tested were from L1-2 to L3-4 levels. Only one was from the L4-5 and none from the L5-S1 levels. The L4-5 and L5-S1 levels are thought to be the site of most low back pathology. Jayson and Barks [5] describe the differences between upper and lower level lumbar disks. They found the lower disk nuclei often to be placed more posteriorly, particularly at L5-S1. This posterior placement of the nucleus is accompanied by an initial posterior bulge. These differences between the upper and lower lumbar level segments should be remembered when intepreting the results of this investigation.

Agreement With Previous Investigations. The present results compare favorably with those obtained in the past. Hirsch and Nachemson [4], Brown, Hansen, and Yorra [3], and Lin, Liu and Adams [6] all obtained bulges resulting from compressive loads similar to those found here. Shah, Hampson, and Jayson [12] obtained slightly different results for compressive loading, but they used a loading system that constrained their vertebrae from shear motions. Brown, Hansen, and Yorra [3] reported values for disk bulge in bending similar to the present, despite their noncompensation for vertebral body translations. They too noted that expansion at some sites around the disk periphery and contraction at others accompanied some modes of bending. They also reported that posterior element removal had minimal effect on bulge. All these researchers found substantial individual variations when comparing among disks, in agreement with present findings. Rolander and Blair [10] also found end plate bulge to be insignificant at the compressive load levels used in the present tests. The values obtained for vertebral body motion and intradiscal pressure are quite similar to those reported by Schultz, et al. [11].

Clinical Implications Concerning Nerve Root Entrapment. The test results have possible clinical implications with regard to the entrapment of lumbar-level spinal nerve roots. These nerve roots leave the cauda equina and course inferiorly and laterally (Fig. 6). They cross posteriorly over one disk, then pass underneath a pedicle, and through the intervertebral foramen. At the point of emergence from the foramen, the nerve root is once again in contact with the disk; this time postererolaterally, and one level down. The nerve roots is then twice exposed to contact with the posterior or posterolateral aspect of a disk and the edges of its adjacent vertebral bodies. The nerve root and soft tissues pass through a channel that typically is about 1 cm in width, measured from

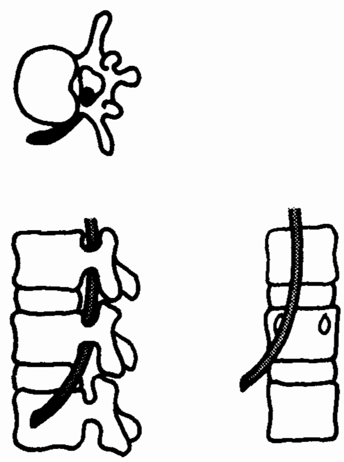

Fig. 6 Schematic diagram of the course of a lumbar region nerve root as it emerges from the spinal canal

the disk to the facet structures. A disk with a large positive bulge may impinge on a nerve root at these contact points. However, a vertebral body edge could also impinge on the root, so that impingment might occur even when disk bulge is zero or negative.

The largest positive posterolateral bulge observed occurred in degenerated segments, some of which bulged as much as 3 mm. Some degenerated segments have vertebral body relative translations that were as large as 5 mm in the posterior direction. Comparing these bulges and translations to a typical channel width of 1 cm, a reduction of 50 percent or more could be caused by vertebral body edge translation, or a combination of translation and disk bulging. In vertebrae with narrower channels, the reduction in the space available for the passage of the nerve root might be even more severe.

Reasonable Assumptions When Modeling the Disk. If disk bulge is to be analyzed via a mechanical model of a motion segment (Belytschko, et al. [2], for example), it would seem safe to omit the posterior elements from the model. The present results show that posterior elements removal has little effect on bulge. Also, since the end plate bulge found in the present tests was insignificant, the assumption of a rigid end plate when modeling behavior at the load levels reported would seem valid.

Conclusions

1 Under compressive loads up to 800 N and moments in flexion, extension, right lateral bending or torsion of up to 11.8 Nm, mean disk bulges of up to 2.7 mm beyond the unloaded-state bulges occur. The largest bulges are produced in right lateral bending.

2 Posterolateral bulges have nearly the same magnitudes as lateral bulges, but posterior bulges are generally smaller.

3 Degenerated disks bulge more than nondegenerated disks under the same load.

4 Fluid injection and posterior element removal have little effect on disk bulge.

5 There is no clear relationship between intradiskal pressure and disk bulge.

6 End plate bulge is small compared to disk bulge, and may be negligible.

7 Since vertebral body edge translation is often as large or larger than disk bulge, nerve root impingement could be caused by this edge translation alone, or by combinations of edge translation and disk bulge.

Acknowledgment

The support of US Public Health Service Grant AM 15575 and OH 00514 and Development Award AM 00029; and the assistance of Karol Haderspeck, Teresa Smith and David Warwick are gratefully acknowledged.

References

1 Andersson, G., and Schultz, A., "Effects of Fluid Injection on Mechanical Properties of Intervertebral Discs," *Journal of Biomechanics*, Vol. 12, 1979, pp. 453-458.

2 Belytschko, T., Kulak, R., Schultz, A., and Galante, J., "Finite Element Stress Analysis of an Intervertebral Disc," *Journal of Biomechanics*, Vol. 7, 1974, pp. 277-285.

3 Brown, T., Hansen, R., and Yorra, A., "Some Mechanical Tests on the Lumbosacral Spine with Particular Reference to the Intervertebral Discs," *Journal of Bone and Joint Surgery*, Vol. 39A, 1957, pp. 1135-1164.

4 Hirsch, C., and Nachemson, A., "New Observations on the Mechanical Behavior of Lumbar Discs," *Acta Orthop. Scand.*, Vol. 23, 1954, pp. 254-283.

5 Jayson, M., and Barks, J., "Structural Changes in Intervertebral Discs," *Annals of Rheumatic Diseases*, Vol. 32, 1973, pp. 10-15.

6 Lin, H., Liu, Y., and Adams, K., "Mechanical Response of the Lumbar Intervertebral Joint Under Physiological (Complex) Loading," *Journal of Bone and Joint Surgery*, Vol. 60A, 1978, pp. 41-55.

7 Nachemson, A., "Lumbar Intradiscal Pressure," *Acta Orthop. Scand.*, Supplement 43, 1960.

8 Nachemson, A., and Elfstrom, G., "Intravital Dynamic Pressure Measurements in Lumbar Discs," *Scandinavian Journal of Rehabilitation Medicine*, Supplement 1, 1970.

9 Reuber, M., "Disc Bulge in Lumbar Intervertebral Discs," Carleton University, (thesis), 1978.

10 Rolander, S., and Blair, W., "Deformation and Fracture of the Lumbar Vertebral End Plate," *Orthopaedic Clinics of North America*, Vol. 6, 1975, pp. 75-81.

11 Schultz, A., Warwick, D., Berkson, M., and Nachemson, A., "Mechanical Properties of Human Lumbar Spine Motion Segments—Part 1: Responses in Flexion, Extension, Lateral Bending, and Torsion," ASME JOURNAL OF BIOMECHANICAL ENGINEERING, Vol. 101, 1979, pp. 46-52.

12 Shah, J., Hampson, W., and Jayson, M., "The Distribution of Surface Strain in the Cadaveric Lumbar Spine," *Journal of Bone and Joint Surgery*, Vol. 60B, 1978, pp. 246-251.

13 Sonada, T., "Studies on the Strength for Compression Tension, and Torsion of the Human Vertebral Column," *Journal of Kyoto Pref. Medical University*, Vol. 71, 1962, pp. 659-702.